applied sciences

MDPI

Article

Nonlinear Adaptive Robust Control of the Electro-Hydraulic Servo System

Lijun Feng and Hao Yan *

School of Mechanical, Electronic and Control Engineering, Beijing Jiaotong University, Beijing 100044, China; 15116334@bjtu.edu.cn

* Correspondence: hyan@bjtu.edu.cn

Received: 14 June 2020; Accepted: 25 June 2020; Published: 29 June 2020

Abstract: This paper focuses on high performance adaptive robust position control of electro-hydraulic servo system. The main feature of the paper is the combination of adaptive robust algorithm with discrete disturbance estimation to cope with the parametric uncertainties, uncertain nonlinearities, and external disturbance in the hydraulic servo system. First of all, a mathematical model of the single-rod position control system is developed and a nonlinear adaptive robust controller is proposed using the backstepping design technique. Adaptive robust control is used to encompass the parametric uncertainties and uncertain nonlinearities. Subsequently, a discrete disturbance estimator is employed to compensate for the effect of strong external disturbance. Furthermore, a special Lyapunov function is formulated to handle unknown nonlinear parameters in the system state equations. Simulations are carried out, and the results validate the superior performance and robustness of the proposed method.

Keywords: nonlinear adaptive robust control; electro-hydraulic system; Lyapunov function; discrete disturbance estimator

1. Introduction

Hydraulic systems are widely used in modern industrial applications such as a parallel robot platform [1], automative suspension system [2], hydraulic load emulator [3], etc., due to their rapid response, high control precision, and large power transmission capability. However, the hydraulic system is always subjected to model uncertainties caused by complex flow–pressure properties of the control valve, oil compressibility, and leakage [4]. In addition, the hydraulic system also contains some hard nonlinearities such as control input saturation, dead zone nonlinear friction, etc. [5]. Due to the presence of high nonlinearities and large uncertainties, it is challenging to design a satisfactory controller for the hydraulic servo system.

During the past two decades, classical control theory and feedback linearization used for the control of the hydraulic system have been studied in [6,7]. These methods performed well under nominal operating conditions. However, in the presence of large uncertainties and unmodeled dynamics, these techniques fail to perform satisfactorily. To attenuate the effect of parametric uncertainties in the hydraulic system, many nonlinear control schemes were proposed, such as adaptive control [8], sliding mode [9], fuzzy logic [10], and neural network control [11]. Adaptive control can reduce the adverse effect of parametric uncertainties, but it could do little to deal with the influence of nonlinear dynamics and external disturbances. Sliding mode control is used to attenuate uncertainties and disturbance, but it contains a fast switching action and large control activities, which may cause system chatter around the desired states. Fuzzy logic control depends heavily on the knowledge of the expert and neural network control needs a huge amount of training data and high computational complexity. Therefore, they are all difficult to implement in practical applications.

To overcome both parametric uncertainties and unknown nonlinearities, adaptive robust control [12], which combines adaptive backstepping control with sliding filter structure, is proposed in [13,14] and is used to deal with the system uncertainties and unmodeled dynamics. This method was thoroughly tested in [15–18], and the results show that it provides excellent performance in terms of both the transient response and the final tracking accuracy even in the presence of parametric uncertainties and uncertain nonlinearities. An adaptive control based on the Udwadia–Kalaba approach is presented to deal with various uncertainties and the external disturbance in rehabilitation robot applications [19]. To mitigate the effect of measurement noise, a desired compensation adaptive robust control is put forward in [20], which uses desired state variables in regressors instead of measured state variables [21]. A control strategy combining integral robust control and desired compensation adaptive robust control for high-precision position control of electro-hydraulic systems is developed and satisfactory performance is obtained [22]. An indirect adaptive robust scheme is presented in [23] that uses the least mean square method to estimate unknown parameters. In [24], a switch strategy is used to select a better control scheme between direct and indirect adaptive control methods. An RBF-neural-network-based adaptive robust control design is proposed for nonlinear bilateral teleoperation manipulators to cope with uncertainty communication time delay in the remote tasks [25]. In [26], a data-based learning adaptive robust control (LARC) strategy based on the gated recurrent unit (GRU) neural network is proposed to achieve accurate tracking error prediction, rigorous motion accuracy, and accurate tracking certain robustness.

In the design process of an adaptive robust controller [27,28], system state equations are usually required to be linearly parametrized by unknown constant parameters. However, the above condition is not satisfied for some mechanical systems such as hydraulic control systems. Existing adaptive robust control schemes cannot solve the problem with the unknown nonlinear parameters. A special Lyapunov function was developed in [29] to convert unknown nonlinear parameters to unknown linear types. However, this control scheme doesn't consider the effect of parameter estimation errors, which may result in system unstability.

In this paper, a nonlinear adaptive robust control for the valve-controlled hydraulic system is developed based on adaptive robust control and discrete disturbance estimation. First of all, the dynamics of hydraulic system are investigated. The uncertainties considered in this paper include unknown linear or the nonlinear parameters. Meanwhile, a nonlinear adaptive robust control law is deduced based on a special Lyapunov function, which not only guarantees the boundedness of state variables and control signal but also compensates for the effect of parameter uncertainties, external disturbance, and errors in parametric estimates. Finally, the proposed control scheme is evaluated by some computer simulations in various working conditions to verify its dynamic performance and robustness.

The paper is organized as follows:. In Section 2, problem formulation and the detailed nonlinear model of the hydraulic system are presented. In Section 3, the proposed nonlinear adaptive robust control with a discrete disturbance estimator is described. In Section 4, computer simulations are executed for evaluating the performance and robustness of the proposed control scheme, and the results are discussed. The conclusions are presented in Section 5.

2. Modeling of the Hydraulic System

The hydraulic system shown in Figure 1 is comprised of a single-rod cylinder, a 4/3- way servo valve, and a mass load. The goal of this paper is to make the mass load track the desired motion trajectory as closely as possible.

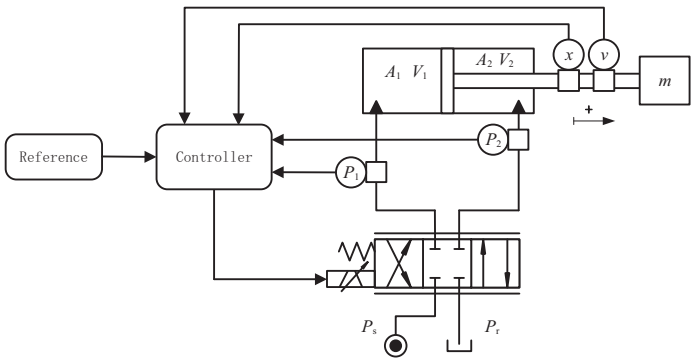

Figure 1. The scheme of the hydraulic system.

The dynamic of the piston can be described as follows::

$$P_1 A_1 - P_2 A_2 = m\ddot{x} + f_L \tag{1}$$

where P_1, P_2 are the pressure in two chambers of cylinder, respectively. A_1, A_2 are the piston area of the two chambers, respectively. m is the mass of load, x is the displacement of load, and f_L is lumped disturbance acting on the cylinder.

Assuming that both the internal leakage f of the servo valve and the external leakage flow of the cylinder have been neglected, then the dynamic of oil flow of the cylinder can be written as

$$\begin{cases} A_1\dot{x} + C_t(P_1 - P_2) + \dfrac{V_{01} + A_1 x}{\beta_e}\dot{P}_1 = Q_1 \\ A_2\dot{x} + C_t(P_1 - P_2) = \dfrac{V_{02} - A_2 x}{\beta_e}\dot{P}_2 + Q_2 \end{cases} \tag{2}$$

where C_t is the coefficient of cylinder internal leakage flow, and β_e is the effective bulk modulus of oil in the container. V_{01}, V_{02} are the original total control volumes of two chambers respectively, which include the volume of the servo valve, pipelines, and cylinder chambers, and $V_1 = V_{01} + A_1 x$, $V_2 = V_{02} - A_2 x$. Q_1 represents the supply flow rate of the forward chamber, and Q_2 represents the return flow rate of the return chamber.

Q_1 and Q_2 are given as

$$\begin{cases} Q_1 = k_q x_v[s(x_v)\sqrt{P_s - P_1} + s(-x_v)\sqrt{P_1 - P_r}] \\ Q_2 = k_q x_v[s(x_v)\sqrt{P_2 - P_r} + s(-x_v)\sqrt{P_s - P_2}] \end{cases} \tag{3}$$

with an index function of valve direction $s(x)$ being defined as

$$s(x) = \begin{cases} 1, & \text{if } x \geq 0 \\ 0, & \text{if } x < 0 \end{cases} \tag{4}$$

where P_s is the system supply pressure and P_r is the container pressure. x_v is the spool displacement of servo valve, k_q is the valve flow gain coefficient and $k_q = C_d w\sqrt{\frac{2}{\rho}}$, in which C_d is the discharge coefficient, w is the spool area gradient, and ρ is the oil fluid density.

A high-performance servo valve having a natural frequency of 80 Hz is used, which is much higher than the frequency of desired motion trajectories. Thus, we can assume that the dynamic of spool displacement is linear with the control input, and the following equation $x_v = \psi u$ is satisfied, where ψ is a positive constant, and u is control input. Meanwhile, $s(x_v) = s(u)$ can be obtained by following the above assumption.

Therefore, Equation (3) can be transformed into

$$\begin{cases} Q_1 = gu[s(u)\sqrt{P_s - P_1} + s(-u)\sqrt{P_1 - P_r}] \\ Q_2 = gu[s(u)\sqrt{P_2 - P_r} + s(-u)\sqrt{P_s - P_2}] \end{cases} \tag{5}$$

where $g = k_q\psi$.

Defining the system state variables as

$$x \triangleq (x_1, x_2, x_3, x_4)^{\mathrm{T}} = (y, \dot{y}, P_1, P_2)^{\mathrm{T}},$$

and

$$\begin{cases} R_1(x) = s(u)\sqrt{P_s - x_3} + s(-u)\sqrt{x_3 - P_r} \\ R_2(x) = s(u)\sqrt{x_4 - P_r} + s(-u)\sqrt{P_s - x_4} \end{cases}$$

then the entire state equations of the hydraulic system can be expressed as follows:

$$\begin{cases} \dot{x}_1 = x_2 \\ \dot{x}_2 = \dfrac{1}{m}\left(A_1 x_3 - A_2 x_4 - f_L\right) \\ \dot{x}_3 = \dfrac{\beta_e}{V_{01} + A_1 x_1}\left[-A_1 x_2 - C_t(x_3 - x_4) + guR_1(x)\right] \\ \dot{x}_4 = \dfrac{\beta_e}{V_{02} - A_2 x_1}\left[A_2 x_2 + C_t(x_3 - x_4) - guR_2(x)\right] \end{cases} \tag{6}$$

To simplify the system state equations, some variables and parameters are defined as follows:

$$\begin{cases} \overline{x}_3 = \dfrac{A_1 x_3 - A_2 x_4}{m} \\ d = -\dfrac{f_L}{m} \\ \beta = \dfrac{A_1 \beta_e}{m} \\ k_A = \dfrac{A_2}{A_1} \end{cases}$$

and the state Equations (6) can be rewritten as

$$\begin{cases} \dot{x}_1 = x_2 \\ \dot{x}_2 = \overline{x}_3 + d \\ \dot{\overline{x}}_3 = \left[\dfrac{\beta}{V_{01} + A_1 x_1} gR_1(x) + \dfrac{k_A \beta}{V_{02} - A_2 x_1} gR_2(x)\right] u + \\ \qquad \dfrac{\beta}{V_{01} + A_1 x_1}[A_1 x_2 - C_t(x_3 - x_4)] - \\ \qquad \dfrac{k_A \beta}{V_{02} - A_2 x_1}[A_2 x_2 + C_t(x_3 - x_4)] \end{cases} \tag{7}$$

Given a bounded desired trajectory $x_d(t) \in \mathbb{C}^3$, the objective of this paper is to design a bounded control input u such that the output x_1 tracks the desired motion trajectory $x_d(t)$ closely in spite of uncertainties and external disturbance. The design of nonlinear adaptive robust controller will be described in the following section.

3. Controller Design

In order to find the correct control input for the hydraulic system, a nonlinear adaptive robust controller is developed for the state Equations (7). Here, we assume that the desired motion trajectory $x_d(t)$, its velocity$\dot{x}_d(t)$, acceleration $\ddot{x}_d(t)$, and the derivate of acceleration $\dddot{x}_d(t)$ exist and are bounded. The procedure for designing the controller based on the backstepping technique is described as follows:

Step 1: define the system output tracking error as

$$z_1 \triangleq x_1 - x_d \tag{8}$$

then the time derivative term of tracking error is calculated as follows:

$$\dot{z}_1 = x_2 - \dot{x}_d \tag{9}$$

Define z_2 as the state error between state variable x_2 and the virtual control x_{2d} as

$$z_2 \triangleq x_2 - x_{2d} \tag{10}$$

Here, treat x_{2d} as a virtual control input for x_2, which is defined as

$$x_{2d} \triangleq \dot{x}_d - k_1 z_1 \tag{11}$$

where k_1 is a positive constant.

Combining (10) and (11), we have

$$\dot{z}_1 = -k_1 z_1 + z_2 \tag{12}$$

Consider a candidate Lyapunov function

$$V_1 = \frac{1}{2} z_1^2 \tag{13}$$

then

$$\dot{V}_1 = z_1 \dot{z}_1 = z_1 z_2 - k_1 z_1^2 \tag{14}$$

It can be found that, if the z_2 is close to zero, the tracking error z_1 will converge to zero as well. Thus, the next step is to design a control law to make z_2 as small as possible.

Step2: Take the derivative of z_2 results in the following equation

$$\dot{z}_2 = \dot{x}_2 - \dot{x}_{2d} = \overline{x}_3 + d - \ddot{x}_d + k_1 \dot{z}_1 \tag{15}$$

A virtual control law $\overline{x}_{3d}$ for Equation (15) is chosen as

$$\overline{x}_{3d} \triangleq \ddot{x}_d - z_1 - k_1 \dot{z}_1 - k_2 z_2 - \hat{d}, \quad k_2 = \frac{H_1^2}{4\delta} + \eta_2 \tag{16}$$

where $\hat{d}$ is the estimate of the disturbance d and the estimate error $\tilde{d}$ is defined as $\tilde{d} \triangleq d - \hat{d}$. η_2 and δ are positive constants and δ is determined by the acceptable bound of z_2. H_1 is the upper bound of $\tilde{d}$ and can be expressed as $H_1 = \sup |\tilde{d}|$.

Since the ideal values of z_1, z_2 and their derivatives are all equal to zero, it is reasonable to construct a discrete disturbance estimator as follows:

$$\hat{d}(k+1) = \ddot{x}_d(k) - \overline{x}_3(k) \tag{17}$$

where k is the kth sample time.

Define the state error z_3 as

$$z_3 \triangleq \overline{x}_3 - \overline{x}_{3d} \tag{18}$$

Consider a candidate Lyapunov function

$$V_2 = V_1 + \frac{1}{2}z_2^2 \tag{19}$$

Then, the time derivative of V_2 is

$$\begin{aligned} \dot{V}_2 &= \dot{V}_1 + z_2\dot{z}_2 = z_2 z_3 - k_1 z_1^2 - \eta_2 z_2^2 - \frac{H_1^2}{4\delta}z_2^2 + z_2\tilde{d} \\ &\leq z_2 z_3 - k_1 z_1^2 - \eta_2 z_2^2 + \delta \end{aligned} \tag{20}$$

It is obvious that, if the value of z_3 is close to zero, z_1 and z_2 will converge to a bounded region determined by $\tilde{d}$ and system initial state values. Thus, the next step is to maintain the value of z_3 close to zero.

Step3: this step is aimed to synthesize an actual control law u for the input of the hydraulic system. For simplicity, the last equation in state Equations (7) can be rewritten as

$$\dot{\overline{x}}_3 = \frac{h_1(x)u + h_2(x)}{g(x)} \tag{21}$$

where

$$\begin{cases} g(x) = (V_{01} + A_1 x_1)(V_{02} - A_2 x_1) \\ \quad\; = V_{01}V_{02} + (V_{02}A_1 - V_{01}A_2)x_1 - A_1 A_2 x_1^2 > 0 \\ h_1(x) = \beta V_{02} g R_1(x) + \beta k_A V_{01} g R_2(x) + \beta g A_2 [R_2(x) - R_1(x)]x_1 \\ h_2(x) = \beta(V_{02} - A_2 x_1)(-A_1 x_2 - C_t(x_3 - x_4)) \\ \quad\; - k_A \beta(V_{01} + A_1 x_1)(A_2 x_2 + C_t(x_3 - x_4)) \\ \quad\; = -C_t\beta(V_{02} + K_A V_{01})(x_3 - x_4) - \beta(V_{02}A_1 + k_A V_{01}A_2)x_2 \\ \quad\; + \beta A_2(A_1 - A_2)x_1 x_2 \end{cases}$$

Here, parametric uncertainties in the hydraulic system are considered as a parametric vector, which is defined as

$$\begin{cases} \alpha \triangleq [\alpha_1 \quad \alpha_2 \quad \alpha_3 \quad \alpha_4 \quad \alpha_5 \quad \alpha_6 \quad \alpha_7 \quad \alpha_8]^{\mathrm{T}} \\ \alpha_1 \triangleq V_{01}V_{02} \\ \alpha_2 \triangleq V_{02}A_1 - V_{01}A_2 \\ \alpha_3 \triangleq \beta V_{02} g \\ \alpha_4 \triangleq \beta k_A V_{01} g \\ \alpha_5 \triangleq \beta g A_2 \\ \alpha_6 \triangleq C_t\beta(V_{02} + k_A V_{01}) \\ \alpha_7 \triangleq \beta(V_{02}A_1 + k_A V_{01}A_2) \\ \alpha_8 \triangleq \beta A_2(A_1 - A_2) \end{cases}$$

For simplicity, define

$$\begin{cases} \alpha_g \triangleq [\alpha_1 \quad \alpha_2 \quad 1]^{\mathrm{T}} \\ \alpha_{h1} \triangleq [\alpha_3 \quad \alpha_4 \quad \alpha_5]^{\mathrm{T}} \\ \alpha_{h2} \triangleq [\alpha_6 \quad \alpha_7 \quad \alpha_8]^{\mathrm{T}} \end{cases}$$

and

$$\begin{cases} \overline{g}(x) \triangleq [1 \quad x_1 \quad -A_1A_2x_1^2]^{\mathrm{T}} \\ \overline{h}_1(x) \triangleq [R_1 \quad R_2 \quad (R_2-R_1)x_1]^{\mathrm{T}} \\ \overline{h}_2(x) \triangleq [x_4-x_3 \quad -x_2 \quad x_1x_2]^{\mathrm{T}} \end{cases}$$

Obviously, the following statements hold:

$$\begin{cases} g(x) = \alpha_g^{\mathrm{T}}\overline{g}(x) \\ h_1(x) = \alpha_{h1}^{\mathrm{T}}\overline{h}_1(x) \\ h_2(x) = \alpha_{h2}^{\mathrm{T}}\overline{h}_2(x) \end{cases} \tag{22}$$

To cope with the effect of parametric estimate error, we assume that an unknown parametric vector always lies in a known bounded region, namely,

$$\alpha \in \Omega_\alpha \triangleq \{\alpha : \alpha_{\min} < \alpha < \alpha_{\max}\}$$

where $\alpha_{\min} = [\alpha_{1\,\min}, \alpha_{2\,\min}, \cdots, \alpha_{8\,\min}]^{\mathrm{T}}$ and $\alpha_{\max} = [\alpha_{1\,\max}, \alpha_{2\,\max} \cdots, \alpha_{8\,\max}]^{\mathrm{T}}$.

Then, Equation (22) can be rewritten as

$$\begin{cases} g(x) = \alpha_1 + \alpha_2x_1 - A_1A_2x_1^2 > 0 \\ h_1(x) = \alpha_3R_1(x) + \alpha_4R_2(x) + \alpha_5[R_2(x) - R_1(x)]x_1 \\ h_2(x) = -\alpha_6(x_3 - x_4) - \alpha_7x_2 + \alpha_8x_1x_2 \end{cases} \tag{23}$$

Since $g(x) > 0$, the Lyapunov function is defined as

$$V_3 = \frac{1}{2}g(x)z_3^2 \tag{24}$$

The time derivative of Equation(24) is calculated as follows:

$$\begin{aligned} \dot{V}_3 &= \frac{1}{2}\dot{g}(x)z_3^2 + g(x)z_3\dot{z}_3 \\ &= \frac{1}{2}\dot{g}(x)z_3^2 + z_3(h_1(x)u + h_2(x) - g(x)\dot{\bar{x}}_{3d}) \end{aligned} \tag{25}$$

Here, the derivative of $\dot{\bar{x}}_3$ can be calculated as

$$\dot{\bar{x}}_{3d} = \dot{\bar{x}}_3 - k_1\dot{z}_1 - \dot{z}_1 - k_2\dot{z}_2 \tag{26}$$

Since $\dot{\bar{x}}_3$ has some uncertain parameters, a sliding mode observer can be used to estimate the derivative of state $\overline{x}_3$, i.e.,

$$\begin{cases} \dot{w}_1 = -\rho(\overline{x}_3, w_1)\mathrm{sign}(\overline{x}_3 - w_1) \\ \hat{\dot{\bar{x}}}_3 = -\dfrac{\rho(\overline{x}_3, w_1)}{s/\tau + 1}\mathrm{sign}(\overline{x}_3 - w_1) \end{cases} \tag{27}$$

where w_1 is the estimate of $\overline{x}_3$, $\rho(\overline{x}_3, w_1) = \beta_{est}e^{0.3|\overline{x}_3 - w_1|}$ is a variable observer gain, and β_{est} is a design parameter. τ is a first-order filter time constant, and s is the Laplace operator. $\hat{\dot{\bar{x}}}_3$ is the estimate of $\dot{\bar{x}}_3$.

The observer can ensure the convergence of w_1 to $\overline{x}_3$ in a finite time t_f , so there exists a bounded positive H_2 such that estimate error $\tilde{\dot{\bar{x}}}_3 \triangleq \dot{\bar{x}}_3 - \hat{\dot{\bar{x}}}_3$ and $H_2 = \sup|\tilde{\dot{\bar{x}}}_3|$, where H_2 is a positive constant.

Let $\hat{\alpha}_g$, $\hat{\alpha}_{h1}$, $\hat{\alpha}_{h2}$ be the estimate of α_g, α_{h1}, α_{h2}, respectively. $\tilde{\alpha}_g \triangleq \alpha_g - \hat{\alpha}_g$, $\tilde{\alpha}_{h1} \triangleq \alpha_{h1} - \hat{\alpha}_{h1}$ and $\tilde{\alpha}_{h2} \triangleq \alpha_{h2} - \hat{\alpha}_{h2}$ are the estimate errors. Then, the control input u is designed as

$$\begin{cases} u = \dfrac{1}{\hat{\alpha}_{h1}^{\mathrm{T}}\bar{h}_1(x)}(u_1 + u_2) \\ u_1 = -\hat{\alpha}_{h2}\bar{h}_2(x) - \dfrac{1}{2}\hat{\alpha}_g^{\mathrm{T}}\dot{\bar{g}}(x)z_3 + \\ \qquad \hat{\alpha}_g^{\mathrm{T}}\bar{g}(x)[(k_1 + k_1^2k_2)z_1 - (k_1k_2 + 1)z_2 + \hat{\dot{x}}_3] \\ u_2 = -z_2 - k_3z_3 \end{cases} \tag{28}$$

where u_1 is the adaptive control input to track the desired trajectory and u_2 is the robust term which deals with parametric estimate errors and external disturbance. k_3 is a positive gain to be determined later. Then, Equation (25) can be written as

$$\dot{V}_3 = z_3[-z_2 - k_3z_3 + \tilde{\alpha}_g^{\mathrm{T}}\phi_g + \tilde{\alpha}_{h1}^{\mathrm{T}}\bar{h}_1(x)u + \tilde{\alpha}_{h2}^{\mathrm{T}}\bar{h}_2(x) + (k_1 + k_2)\alpha_g^{\mathrm{T}}\bar{g}(x)\tilde{d} - \alpha_g^{\mathrm{T}}\bar{g}(x)\tilde{\dot{x}}_3] \tag{29}$$

where $\phi_g \triangleq \dfrac{1}{2}\dot{\bar{g}}(x)z_3 - \bar{g}(x)[(k_1 + k_1^2k_2)z_1 - (k_1k_2 + 1)z_2 + \hat{\dot{x}}_3]$ and $k_3 = \eta_3 + h(x,u)$. $h(x,u)$ can be defined as follows:

$$\begin{aligned} h(x,u) \triangleq & \frac{1}{4\varepsilon_g}\|\alpha_{gM}\|^2\|\phi_g\|^2 + \frac{1}{4\varepsilon_{h_1}}\|\alpha_{h_1M}\|^2\|\bar{h}_1u\|^2 + \frac{1}{4\varepsilon_{h_2}}\|\alpha_{h_2M}\|^2\|\bar{h}_2\|^2 \\ & + \frac{1}{4\varepsilon_d}(k_1 + k_2)^2H_1^2\|\alpha_{g\max}\|^2\|\bar{g}(x)\|^2 + \frac{1}{4\varepsilon_e}H_2^2\|\alpha_{g\max}\|^2\|\bar{g}(x)\|^2 \end{aligned}$$

where $\alpha_{gM}, \alpha_{h_1M}$ and α_{h_2M} are the absolute error limits, respectively. $\alpha_{gM} = \alpha_{g\max} - \alpha_{g\min}$, $\alpha_{h_1M} = \alpha_{h_1\max} - \alpha_{h_1\min}$ and $\alpha_{h_2M} = \alpha_{h_2\max} - \alpha_{h_2\min}$. ϵ_g , ϵ_{h_1}, ϵ_{h_2}, ϵ_d and ϵ_e are the design positive constants such that $\varepsilon = \varepsilon_g + \varepsilon_{h_1} + \varepsilon_{h_2} + \varepsilon_d + \varepsilon_e$.

In order to consider the effect of parametric uncertainties in the hydraulic system, an augmented Lyapunov function V_a is designed as

$$V_a = V_2 + V_3 + \frac{1}{2}\left(\tilde{\alpha}_g^{\mathrm{T}}T_g^{-1}\tilde{\alpha}_g + \tilde{\alpha}_{h1}^{\mathrm{T}}T_{h1}^{-1}\tilde{\alpha}_{h1} + \tilde{\alpha}_{h2}^{\mathrm{T}}T_{h2}^{-1}\tilde{\alpha}_{h2}\right) \tag{30}$$

where T_g, T_{h1} and T_{h2} are the positive definite constant diagonal matrices. Then, the time derivative of Equation (30) is calculated as

$$\begin{aligned} \dot{V}_a &= \dot{V}_2 + \dot{V}_3 - \left(\tilde{\alpha}_g^{\mathrm{T}}T_g^{-1}\dot{\hat{\alpha}}_g + \tilde{\alpha}_{h1}^{\mathrm{T}}T_{h1}^{-1}\dot{\hat{\alpha}}_{h1} + \tilde{\alpha}_{h2}^{\mathrm{T}}T_{h2}^{-1}\dot{\hat{\alpha}}_{h2}\right) \\ &= -k_1z_1^2 - \eta_2z_2^2 + z_2\tilde{d} - \frac{H_1^2}{4\delta}z_2^2 - k_3z_3^2 - (k_1 + k_2)\alpha_g^{\mathrm{T}}\bar{g}(x)\tilde{d} + \alpha_g^{\mathrm{T}}\bar{g}(x)\tilde{\dot{x}}_3 \\ &\quad + \tilde{\alpha}_g^{\mathrm{T}}\left(z_3\phi_g - T_g^{-1}\dot{\hat{\alpha}}_g\right) + \tilde{\alpha}_{h1}^{\mathrm{T}}\left(z_3\bar{h}_1(x)u - T_{h1}^{-1}\dot{\hat{\alpha}}_{h1}\right) \\ &\quad + \tilde{\alpha}_{h2}^{\mathrm{T}}\left(z_3\bar{h}_2(x) - T_{h2}^{-1}\dot{\hat{\alpha}}_{h2}\right) \end{aligned} \tag{31}$$

In order to account for the effect of parametric uncertainties, adaptive update laws can be chosen so that these inequalities hold:

$$\begin{cases} \tilde{\alpha}_g^{\mathrm{T}}\left(z_3\phi_g - T_g^{-1}\dot{\hat{\alpha}}_g\right) \leqslant 0 \\ \tilde{\alpha}_{h1}^{\mathrm{T}}\left(z_3\bar{h}_1(x)u - T_{h1}^{-1}\dot{\hat{\alpha}}_{h1}\right) \leqslant 0 \\ \tilde{\alpha}_{h2}^{\mathrm{T}}\left(z_3\bar{h}_2(x) - T_{h2}^{-1}\dot{\hat{\alpha}}_{h2}\right) \leqslant 0 \end{cases} \tag{32}$$

Then, the adaptation laws for uncertain terms are designed as follows:

$$\begin{cases} \dot{\hat{\alpha}}_g = T_g z_3 \phi_g \\ \dot{\hat{\alpha}}_{h1} = T_{h1} z_3 \bar{h}_1 u \\ \dot{\hat{\alpha}}_{h2} = T_{h2} z_3 \bar{h}_2 \end{cases} \tag{33}$$

Since the parametric vectors are within known boundness, a simple discontinue projection can be used such that

$$\text{proj}_{\alpha}\{*\} = \begin{cases} 0, \text{ if } \hat{\alpha}_i = \alpha_{imax} \text{ and } * > 0 \\ 0, \text{ if } \hat{\alpha}_i = \alpha_{imin} \text{ and } * < 0 \\ *, \text{ otherwise} \end{cases} \tag{34}$$

and the adaptive laws become

$$\begin{cases} \dot{\hat{\alpha}}_g = \text{proj}_{\hat{\alpha}_g}[T_g z_3 \phi_g] \\ \dot{\hat{\alpha}}_{h1} = \text{proj}_{\hat{\alpha}_{h1}}[T_{h1} z_3 \bar{h}_1 u] \\ \dot{\hat{\alpha}}_{h2} = \text{proj}_{\hat{\alpha}_{h2}}[T_{h2} z_3 \bar{h}_2] \end{cases} \tag{35}$$

Obviously, the projection in Equation (34) satisfies the inequalities in Equations (32), which has been proved in [30]. From Equations (28), (31), and (34), one can obtain that

$$\begin{aligned} \dot{V}_a \leqslant & -k_1 z_1^2 - \eta_2 z_2^2 - \eta_3 z_3^2 - \frac{1}{4\varepsilon_g}\|\alpha_{gM}\|^2 \|\phi_g\|^2 z_3^2 - \frac{1}{4\varepsilon_{h_1}}\|\alpha_{h_1 M}\|^2 \|\bar{h}_1\|^2 z_3^2 - \frac{1}{4\varepsilon_{h_2}}\|\alpha_{h_2 M}\|^2 \|\bar{h}_2\|^2 z_3^2 \\ & + \quad z_2 H_1 - \frac{H_1^2}{4\delta} z_2^2 + (k_1 + k_2)\alpha_g^{\mathrm{T}} \bar{g}(x) H_1 z_3 \text{sign}(z_3) - \frac{1}{4\varepsilon_d}(k_1 + k_2)^2 H_1^2 \|\alpha_{g\max}\|^2 \|\bar{g}(x)\|^2 z_3^2 \\ & + \alpha_g^{\mathrm{T}} \bar{g}(x) H_2 z_3 \text{sign}(z_3) - \frac{1}{4\varepsilon_e} H_2^2 \|\alpha_{gM}\|^2 \|\bar{g}(x)\|^2 z_3^2 \\ \leqslant & -k_1 z_1^2 - \eta_2 z_2^2 - \eta_3 z_3^2 - \frac{1}{4\varepsilon_g}\|\alpha_{gM}\|^2 \|\phi_g\|^2 z_3^2 - \frac{1}{4\varepsilon_{h_1}}\|\alpha_{h_1 M}\|^2 \|\bar{h}_1\|^2 z_3^2 - \frac{1}{4\varepsilon_{h_2}}\|\alpha_{h_2 M}\|^2 \|\bar{h}_2\|^2 z_3^2 \\ & + \delta + \varepsilon_d + \varepsilon_e. \end{aligned} \tag{36}$$

which leads to the result that all signals z_1, z_2, z_3, $\tilde{\alpha}_g$, $\tilde{\alpha}_{h1}$, $\tilde{\alpha}_{h2}$, $\hat{\alpha}_g$, $\hat{\alpha}_{h1}$, $\hat{\alpha}_{h2}$ are bounded and

$$V_a \leqslant exp(-\lambda t) V_a(0) + \frac{k}{\lambda}[1 - \exp(-\lambda t)] \tag{37}$$

where $\lambda = min\left\{2k_1, 2\eta_2, 2[(\eta_3 + \frac{1}{4\varepsilon_g}\|\alpha_{gM}\|^2 \|\phi_g\|^2 + \frac{1}{4\varepsilon_{h_1}}\|\alpha_{h_1 M}\|^2 \|\bar{h}_1\|^2 + \frac{1}{4\varepsilon_{h_2}}\|\alpha_{h_2 M}\|^2 \|\bar{h}_2\|^2)]/(\|\alpha_g\| \|\bar{g}(x)\|)\right\}$ and $k = \delta + \varepsilon_d + \varepsilon_e$. Furthermore, if $\tilde{d}$ and $\tilde{\bar{x}}_3$ are both equal zero after a time $t_f > 0$, then the time derivative of V_a satisfies

$$\dot{V}_a \leqslant W, \quad t \geqslant t_f \tag{38}$$

where $W = -k_1 z_1^2 - k_2 z_2^2 - k_2 z_3^2$. Since $W \in L_2$ and $V_a \in L_\infty$, using the Barbalet's lemma, one can conclude that $W \to 0$ as $t \to 0$. Thus, z_1, z_2 and z_3 converge to zero as $t \to \infty$.

Finally, we can conclude that, given a nonlinear system of equations with uncertainties and disturbance as in Equation (7), employing the controller Equation (28), all signals z_1, z_2, z_3, $\tilde{\alpha}_g$, $\tilde{\alpha}_{h1}$, $\tilde{\alpha}_{h2}$, $\hat{\alpha}_g$, $\hat{\alpha}_{h1}$, $\hat{\alpha}_{h2}$ are bounded. Furthermore, after a finite time t_f, if only the parametric uncertainties exist, then zero tracking errors can also be obtained.

Remark: If adaption laws are removed (i.e., T_g, T_{h1}, $T_{h2}2$ are all equal to zero) or the estimation errors are too large, the proposed control scheme can still make all the signals bounded

and $V_a \leqslant exp(-\lambda_v t)V_a(0) + \frac{k_v}{\lambda_v}[1 - \exp(-\lambda_v t)]$, where $\lambda_v = min\left\{2k1, 2\eta_2, 2\eta_3/(\|\alpha_g\|\|\overline{g}(x)\|)\right\}$ and $k_v = \delta + \varepsilon$.

4. Simulation and Discussion

4.1. Simulation Parameters

In order to evaluate the tracking accuracy and robustness of the proposed control scheme for the electro-hydraulic system, three different working conditions are considered, i.e., no load condition, sudden load condition, and load condition with parameter variations. The simulations are conducted on an integrated simulation platform that uses MATLAB and Amesim. The simulation parameters are described as follows:

The supply pressure of pump is set at 10 Mpa by a relief valve and the return pressure of hydraulic system is set at 0 Mpa. The dimensions of cylinder are 80 mm/45 mm/500 mm and the control input of the servo valve is in the range of $[-10, +10]$ mA. The system state variables, which include load position x, velocity v, and the chamber pressures P_1 and P_2 of two cylinder chambers are discretely measured using the sensors in Amesim software. All of the pressure signals are processed through a low-pass filter with 10 Hz cut-off frequency. The control algorithm is implemented in MATLAB and the system sample time is taken as 0.001 s.

The nominal load mass m is 20 kg and the effective bulk modulus of oil fluid is 1.4 Gpa. The coefficient of cylinder internal leakage C_t is 2×10^{-15} (m^3s^{-1}/Pa) and servo valve flow gain g is 5.82×10^{-8} $m^3s^{-1}/(V\sqrt{P_a})$. The original position of piston is in the middle of cylinder and the original control volumes of cylinder chambers are $V_1 = 1.3\times 10^{-3}$ m^3 and $V_2 = 8.89 \times 10^{-4}$ m^3, respectively.

To verify the performance of the designed controller, the proposed nonlinear adaptive robust controller (NARC) is compared with the PID controller and determined robust controller (DRC). The control parameters of the proposed controller are selected as $k_1 = 150$, $\eta_2 = 40$, $H_1 = 2.5$, $\delta = 0.01$, $\beta_{est} = 1$, $\tau = 10$, $H_2 = 1$, $\eta_3 = 20$, $\varepsilon_g = \varepsilon_{h1} = \varepsilon_{h2} = \varepsilon_d = \varepsilon_e = 0.001$, $T_g = diag\{[10^{-8}, 10^{-8}, 0]^{\mathrm{T}}\}$, $T_{h1} = diag\{[10^{-8}, 10^{-8}, 10^{-8}]^{\mathrm{T}}\}$ and $T_{h2} = diag\{[10^{-15}, 10^{-3}, 10^{-3}]^{\mathrm{T}}\}$. The control parameters of determined robust control are the same as that of the proposed controller except that $T_g = diag\{[0, 0, 0]^{\mathrm{T}}\}$, $T_{h1} = diag\{[0, 0, 0]^{\mathrm{T}}\}$ and $T_{h2} = diag\{[0, 0, 0]^{\mathrm{T}}\}$. The range limits of parameters used in DRC and NARC are $\pm$20% of their nominal values. The initial value of parameter estimates are taken as their nominal value. While the control parameters of PID controller are chosen as $K_P = 150$, $K_I = 1$, and $K_D = 0.2$ by trial and error.

4.2. Simulation Results

4.2.1. Case 1: No Load Condition

In this case, there is no load nor there is any variation in the parameters. The desired trajectory is selected as a sinusoidal signal whose amplitude is 50 mm and its frequency is 0.1 Hz. The reference signal is $x_d = 50\sin(0.2\pi t)$ [mm] .

Figure 2 shows the comparison of tracking performances obtained using the PID controller, the DRC, and the proposed nonlinear adaptive robust controller. It is evident that the PID controller presents some lag in tracking the reference signal while DRC and NARC can track the reference signal exactly. The errors in tracking using the three different controllers are shown in Figure 3. It can be observed that, compared with the PID controller, DRC and NARC controllers have smaller tracking error and better dynamic performance. However, there is a small jitter when the DRC and NARC are used.

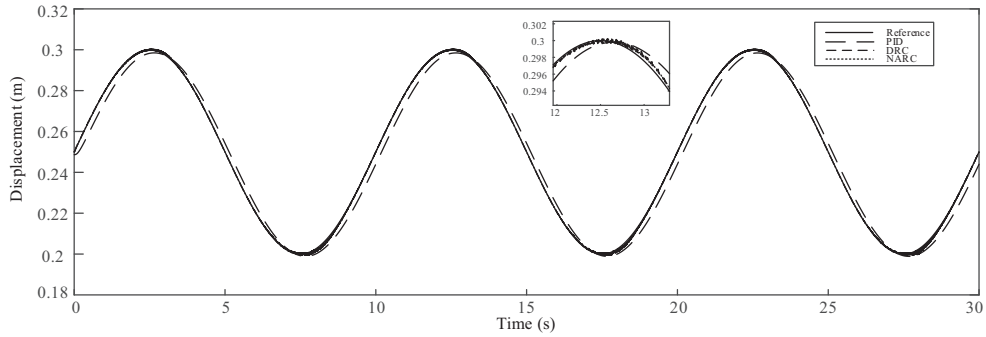

Figure 2. Comparison tracking performance with no load conditon.

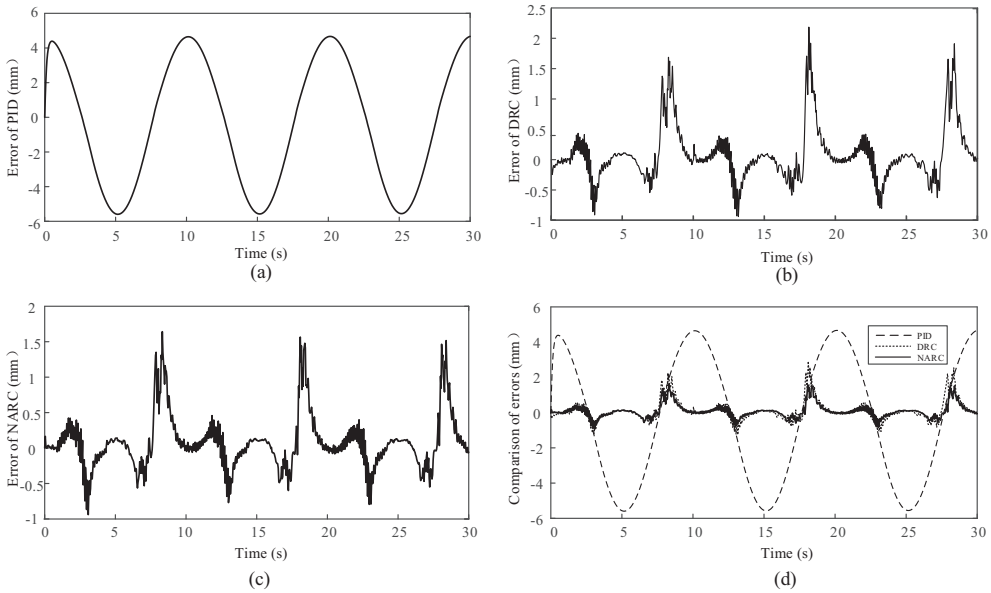

Figure 3. Tracking errors with no load condition, (**a**) tracking error of PID; (**b**) tracking error of DRC; (**c**) tracking error of NARC; (**d**) comparison of tracking errors with the above controllers.

In order to evaluate the effectiveness of the proposed controller under a load disturbance, a sudden load of $d = 250$ is added to system at $t = 10$ s. The corresponding tracking response with three different controllers are shown in Figure 4. As shown in Figure 4, when the sudden load is applied, some tracking fluctuation can be seen with the PID controller. However, the tracking performance of DRC and NARC is largely unaffected. The strong robustness of DRC and NARC is attributed to the exact estimate of disturbance with a discrete disturbance estimator. The tracking errors under a sudden load disturbance with different controllers are shown in Figure 5. It can also be seen that the tracking error with PID is larger than that obtained with the DRC and NARC, which further confirms that the DRC and NARC are more robust than the PID controller because of the discrete disturbance estimator.

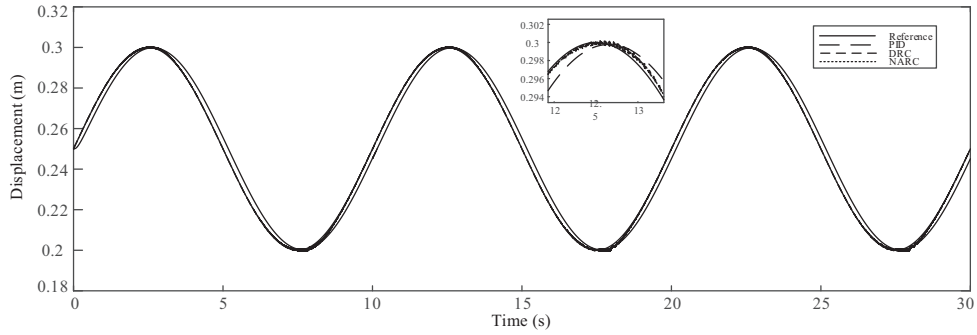

Figure 4. Comparison tracking performance with sudden load at 10 s.

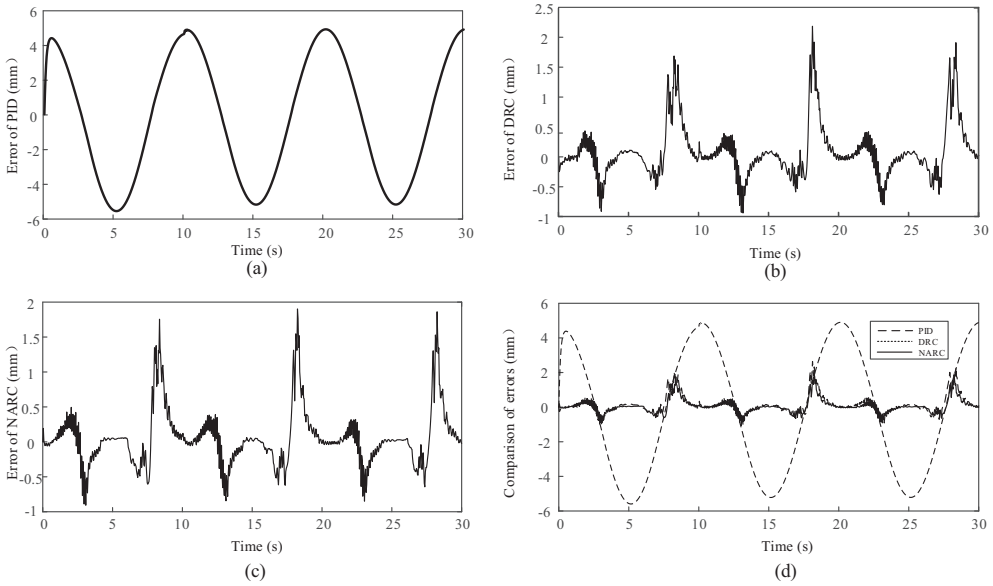

Figure 5. Tracking errors with sudden load condition, (**a**) tracking error of PID; (**b**) tracking error of DRC; (**c**) tracking error of NARC; (**d**) comparison of tracking errors with the above controllers.

4.2.2. Case 2: Sudden Load Condition

The simulations are also carried out to verify the convergence of the NARC under load condition with parameter variations. In simulations, some parameters of the system are changed. The initial displacement of cylinder is changed to 0.247 m. The initial volume of left cylinder chamber is changed to $V_1 = 1.3 \times 10^{-3}$ m^3 and the initial volume of right cylinder chamber is changed to $V_2 = 8.9 \times 10^{-4}$ m^3. The bulk volume of oil is changed to 1.5 Gpa .

Figure 6 shows the tracking performance with the three different controllers with parameter variation and load disturbance. The tracking performance of NARC is not better than the other controllers at the beginning. However, the tracking error decreases slowly with time due to the adaptation rate laws as shown in Figure 7. The parameter estimates are shown in Figure 8. It can be seen that, even though the parameters don't converge to their actual value, they are all bounded and are adjusted to improve the tracking performance. Moreover, the estimate value of load d is almost equal to its actual value as shown in Figure 8, which proves the effectiveness of the discrete disturbance estimator.

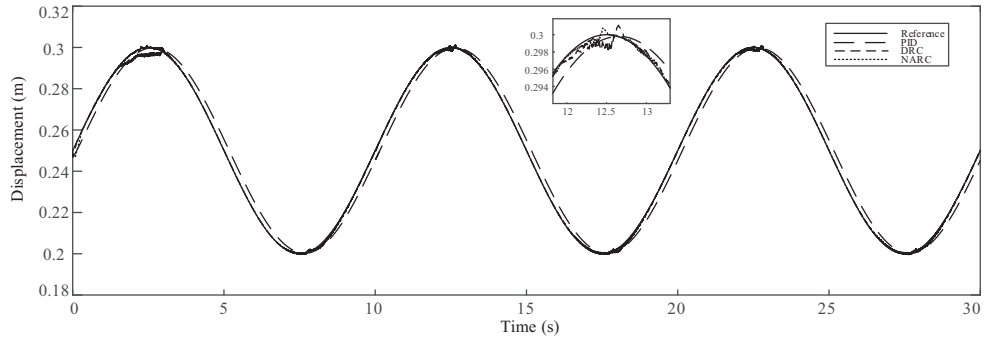

Figure 6. Comparison tracking performance with parameter variations and load conditon.

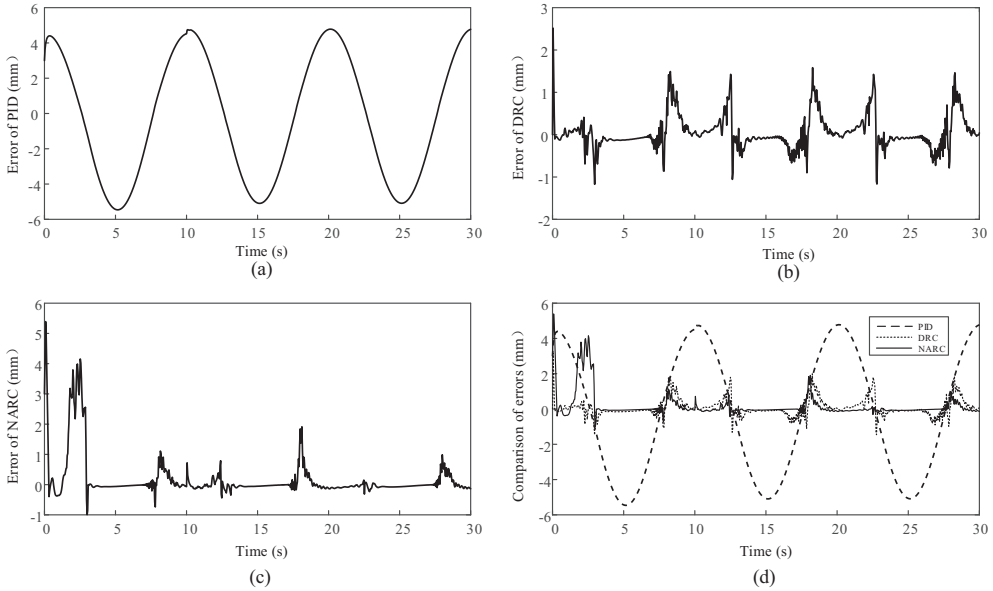

Figure 7. Tracking errors with parameter variation and load condition, (**a**) tracking error of PID; (**b**) tracking error of DRC; (**c**) tracking error of NARC; (**d**) comparison of tracking errors with the above controllers.

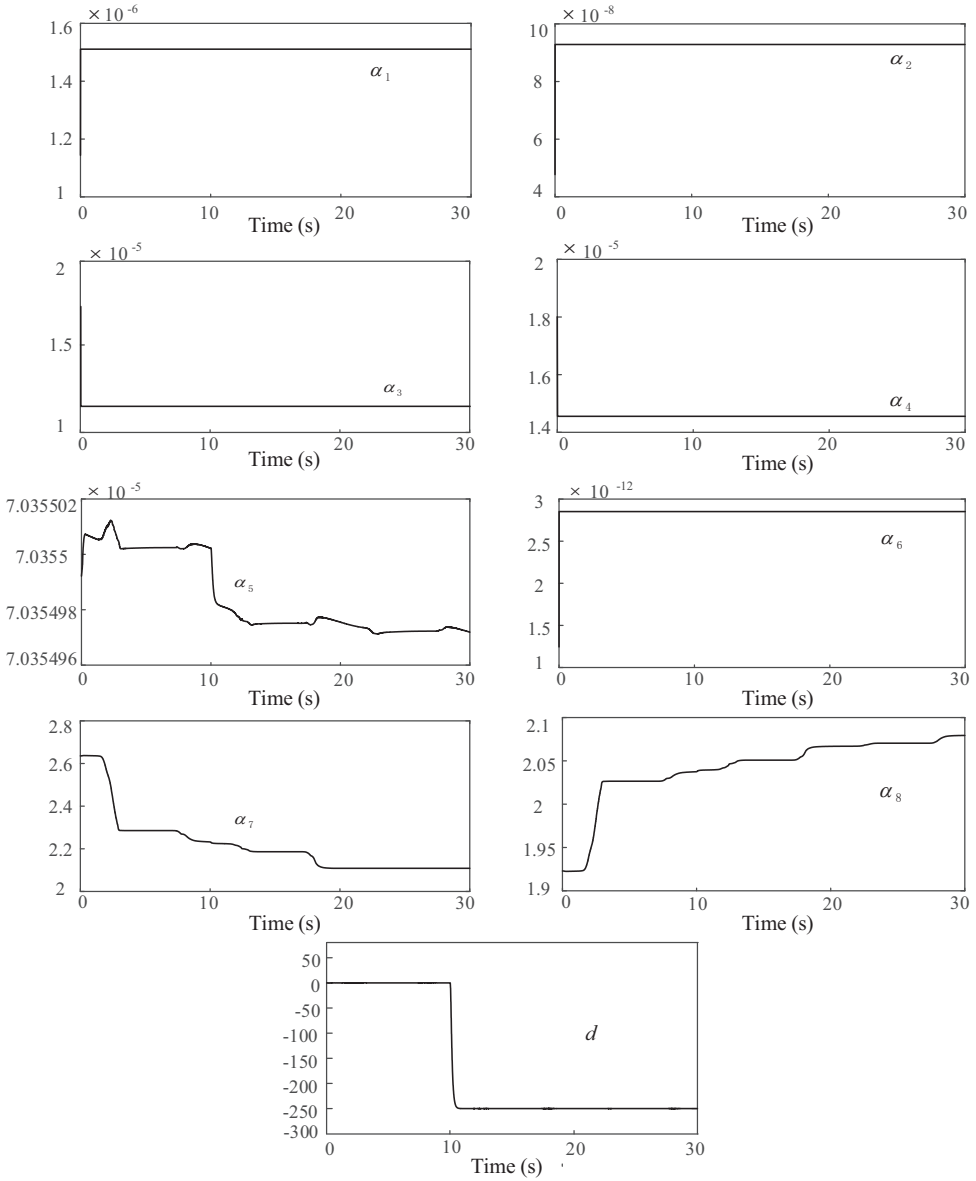

Figure 8. The parameter estimate of the NARC controller.

4.2.3. Case 3: Parameter Variations and Load Disturbance Condition

In order to compare the performance of the three kinds of controllers under different conditions, the maximum tracking error M, the average tracking errors μ and the tracking lag ϕ are statistically analyzed, and results are shown in Table 1. It can be seen from the results that the PID controller can not deal with highly nonlinear parameters and disturbance, and the system control response is so slow that it could not track the reference signal accurately. The maximum tracking error is about 4.8 mm, and the average tracking error is about 3.2 mm. The tracking lag was also apparent than the other controller in all conditions. In addition, the dynamic performance of DRC and NARC are similar under nominal and sudden load conditions because of the same control structure. However, in the variation and load condition, the average tracking error of NARC is 0.126 mm, which is much better than the other controller with the help of the adaptive laws.

Table 1. Performance indexes of controllers under differential conditions.

Controller	Nominal Condition			Sudden Load Condition			Variation and Load Conditon		
	M/mm	μ/mm	ϕ/°	M/mm	μ/mm	ϕ/°	M/mm	μ/mm	ϕ/°
PID	4.7	3.2	5.4	4.9	3.2	5.9	4.8	3.2	6.1
DRC	2.7	0.27	0.07	2.4	0.275	0.0757	3.2	0.28	0.085
NARC	1.8	0.25	0.06	2.4	0.263	0.061	5.6	0.126	0.055

Based on these simulation results, it can be concluded that the NARC can improve the system dynamic performance and can reject external load disturbance effectively.

5. Conclusions

A nonlinear adaptive robust controller has been presented for the electro-hydraulic system driven by a single-rod actuator with uncertain nonlinear parameters, and external disturbance. The effect of unknown nonlinear parameters and external disturbance is considered, and a stable controller is developed using a special Lyapunov function. The whole system controller and adaptation laws are given by combining adaptive robust control and a discrete disturbance estimator, which can compensate for unknown nonlinear parameters, uncertain nonlinearities and external disturbance. The simulation results show that the proposed control achieves a more accurate tracking performance and small tracking lag, under various conditions, which is very important in the high-performance motion control fields.

Author Contributions: L.F. and H.Y. conceived and designed the study. L.F. performed the controller design, carried out simulations and wrote the original draft. H.Y. reviewed and edited the the manuscript. All authors read and approved the manuscript. All authors have read and agreed to the published version of the manuscript.

Funding: This research was funded by the National Natural Science Foundation of China, Grant No. 51775032 and Foundation of Key Laboratory of Vehicle Advanced Manufacturing, Measuring and Control Technology, Beijing Jiaotong University, Ministry of Education, China and Fundamental Research Funds for the Central Universities Grant No. 2017YJS169.

Conflicts of Interest: The authors declare no conflict of interest. The funders had no role in the design of the study; in the collection, analyses, or interpretation of data; in the writing of the manuscript, or in the decision to publish the results.

References

1. Novak, N.; Vladimir, S.; Vladimir, D. Optimal control of hydraulically driven parallel robot platform based on firefly algorithm. *Nonlinear Dyn.* **2015**, *82*, 1457–1473.
2. Jagat, J.R.; Michael, D.; Hamid, R.K.; Kalyana, C.V. Output feedback active suspension control with higher order terminal sliding mode. *IEEE Trans. Ind. Electron.* **2017**, *64*, 1392–1403.
3. Yao, J.Y.; Jiao, Z.X.; Ma, D.W. High dynamic adaptive robust control of load emulator with output feedback signal. *J. Frankl. Inst.* **2014**, *351*, 4415–4433. [CrossRef]
4. Ye, Y.; Yin, C.B.; Gong, Y.; Zhou, J.J. Position control of nonlinear hydraulic system using an improved PSO based PID controller. *Mech. Syst. Signal Pr.* **2017**, *83*, 241–259. [CrossRef]
5. Yao, B.; Bu, F.P.; John, R.; George, T.C. Adaptive robust motion control of single-rod hydraulic actuators: Theory and experiments. *IEEE-ASME Trans. Mech.* **2000**, *5*, 79–91.
6. Honorine, A.M.; Ravinder, V.; Jean-Pierre, K.; Christian, B.. Feedback linearization-based position control of an electrohydraulic servo system with supply pressure uncertainty. *IEEE Trans. Control. Syst. Technol.* **2012**, *20*, 1092–1099.
7. Denis, G.; Krishnaswamy, S. Application of nonlinear adaptive control techniques to an electrohydraulic velocity servomechanism. *IEEE Trans. Control Syst. Technol.* **2004**, *12*, 303–314.
8. Andrew, A.; Liu, R. A simplified approach to force control for electro-hydraulic systems. *Control Eng. Pract.* **2000**, *8*, 1347–1356.

9. Guan, C.; Pan, S.X. Adaptive sliding mode control of electro-hydraulic system with nonlinear unknown parameters. *Control Eng. Pract.* **2008**, *16*, 1275–1284. [CrossRef]
10. Mete, K.; Mustafa, H. Mathematical modelling and fuzzy logic based position control of an electrohydraulic servosystem with internal leakage. *Mechatronics* **2009**, *19*, 847–858.
11. Han, M.K.; Sung, H.P.; Ji, M.L.; Jong, S.K. A robust control of electro hydrostatic actuator using the adaptive back-stepping scheme and fuzzy neural networks. *Int. J. Precis. Eng. Man.* **2010**, *11*, 227–236.
12. Yao, B.; Masayoshi, T. Adaptive robust control of SISO nonlinear systems in a semi-strict feedback form. *Automatica* **1997**, *33*, 893–900. [CrossRef]
13. Yao, B. High performance adaptive robust control of nonlinear systems: A general framework and new schemes. In Proceedings of the 36th IEEE Conference on Decision and Control, San Diego, CA, USA, 12 December 1997; pp. 2489–2494.
14. Tan, Y.L.; Chang, J.; Tan, H.L. Adaptive backstepping control and friction compensation for AC servo with inertia and load uncertainties. *IEEE Trans. Ind. Electron.* **2003**, *50*, 944–952.
15. Yao, B.; Xu, L. Adaptive robust motion control of linear motors for precision manufacturing. *Mechatronics* **2002**, *12*, 595–616. [CrossRef]
16. Yao, J.Y.; Jiao, Z.X.; Ma, D.W. Extended-state-observer-based output feedback nonlinear robust control of hydraulic systems with backstepping. *IEEE Trans. Ind. Electron.* **2014**, *61*, 6285–6293. [CrossRef]
17. Meng, D.Y.; Tao, G.L.; Liu, H.; Zhu, X.C. Adaptive robust motion trajectory tracking control of pneumatic cylinders with LuGre model-based friction compensation. *Chin. J. Mech. Eng.* **2014**, *27*, 802–815. [CrossRef]
18. Yao, J.Y.; Jiao, Z.X.; Yao, B. Nonlinear adaptive robust backstepping force control of hydraulic load simulator: Theory and experiments. *J. Mech. Sci. Technol.* **2014**, *28*, 1499–1507. [CrossRef]
19. Qin, F.; Zhao, H.; Zhen, S.C.; Zhang, Y. Adaptive robust control for lower limb rehabilitation robot with uncertainty based on Udwadia-Kalaba approach. *Adv. Robot.* **2020**, 1–11. [CrossRef]
20. Xu, L.; Yao, B. Adaptive robust precision motion control of linear motors with negligible electrical dynamics: theory and experiments. *IEEE-ASME Trans. Mech.* **2002**, *6*, 444–452.
21. Yao, J.Y.; Deng, W.X.; Sun, W.C. Precision motion control for electro-hydraulic servo systems with noise alleviation: a desired compensation adaptive approach. *IEEE-ASME Trans. Mech.* **2017**, *22*, 1859–1868. [CrossRef]
22. Yang, G.; Yao, J.Y. High-precision motion servo control of double-rod electro-hydraulic actuators with exact tracking performance. *ISA Trans.* **2020**. [CrossRef] [PubMed]
23. Claude, K.; Jean, P.K.; Maarouf, S. Indiscrete adaptive control of an electrohydraulic servo system based on nonlinear backstepping. *IEEE-ASME Trans. Mech.* **2011**, *16*, 1171–1177.
24. Zhang, G.Z.; Chen, J.; Li, Z. Identifier-based adaptive robust control for servomechanisms with improved transient performance. *IEEE Trans. Ind. Electron.* **2010**, *57*, 2536–2547. [CrossRef]
25. Chen, Z.; Sun, W.C.; Gu, J.; Yao, B. RBF-Neural-Network-Based Adaptive Robust Control for Nonlinear Bilateral Teleoperation Manipulators With Uncertainty and Time Delay. *IEEE-ASME Trans. Mech.* **2020**, *25*, 906–918. [CrossRef]
26. Hu, C.; OU, T.S.; Zhu, Y.; Zhu, L.M. GRU-type LARC strategy for precision motion control with accurate tracking error prediction. *IEEE Trans. Ind. Electron.* **2020**. [CrossRef]
27. Yao, J.Y.; Jiao, Z.X.; Han, S.S. Friction compensation for low velocity control of hydraulic flight motion simulator: A simple adaptive robust approach. *Chin. J. Aeronaut.* **2013**, *26*, 814–822. [CrossRef]
28. Yao, J.Y.; Jiao, Z.X.; Ma, D.W.; Yan, L. High-accuracy tracking control of hydraulic rotary actuators with modeling uncertainties. *IEEE-ASME Trans. Mech.* **2014**, *19*, 633–640. [CrossRef]
29. Guan, C.; Pan, S.X. Nonlinear adaptive robust control of single-rod electro-hydraulic actuator with unknown nonlinear parameters. *IEEE Trans. Control Syst. Technol.* **2008**, *16*, 434–445. [CrossRef]
30. Kyoung, K.A.; Doan, N.C.N.; Jin, M.L. Adaptive backstepping control of an electrohydraulic actuator. *IEEE-ASME Trans. Mech.* **2014**, *19*, 987–995.